# Nuclear magnetic resonance force microscopy at millikelvin temperatures

Haan, A.M.J. den

# Chapter 8

# Radio frequency pulses for nuclear magnetic resonance force microscopy

Radio frequent pulses are one of the crucial ingredients in magnetic resonance force microscopy. The magnitude of the spin signal is influenced by the used RF pulse sequence. Moreover, issues involving spurious crosstalk, heat dissipation, and incomplete inversions are important considerations in designing the pulse. In this chapter, several radio frequent pulses, used in NMR and MRFM will be discussed.

As discussed in Chapter 3, in MRFM one can focus either on creating a force interaction or a gradient force interaction between the spins and the magnetic particle of the cantilever. This requires different RF pulses according to the desired interaction. The goal of this chapter is to provide a basic and intuitive understanding of the ways to influence spins, which may be relevant for designing new experiments, especially in our group. In addition, we propose a pulse sequence which is used in NMR and MRI, which may be useful for MRFM experiments in which $T_2$ measurements are relevant.

In the first sections the motion of a (classical) magnetic moment, with only an external magnetic field (section 8.1) and with time varying magnetic field (section 8.2 and section 8.3) will be described. These sections form a foundation for the explanation of common RF pulses (section 8.4) and adiabatic inversions (section 8.5). In section 8.6, the pulse sequence called $B_1$ Insensitive Rotation (BIR) will be described. In the final sections (sections 8.7, 8.8 and 8.9), the use of adiabatic pulses in MRFM and relevant pulses for our group will be discussed.

## 8.1 The motion of a magnetic moment in an external magnetic field

In the following part, we will use a semiclassical description. Further, we will assume that the spins are not interacting and that no dissipation channels are present. The

equation of motion for a magnetic moment $\boldsymbol{\mu}$ in an external magnetic field $\mathbf{B}$ is found by equating the torque $\boldsymbol{\mu} \times \mathbf{B}$ and the rate of change of the angular momentum $\mathbf{J}$:

$$\frac{d\mathbf{J}}{dt} = \boldsymbol{\mu} \times \mathbf{B} \tag{8.1}$$

Hence, since $\boldsymbol{\mu} = \gamma \mathbf{J}$:

$$\frac{d\boldsymbol{\mu}}{dt} = \boldsymbol{\mu} \times \gamma \mathbf{B} \tag{8.2}$$

where $\gamma$ is the gyro-magnetic ratio. Since the direction of change is perpendicular to both $\boldsymbol{\mu}$ and $\mathbf{B}$, the magnetic moment vector will precess around the external magnetic field, thereby describing a cone. Note that the initial angle between the magnetic moment and the external field remains fixed during precession. The frequency at which the magnetic moment precesses around the magnetic field is called the Larmor frequency, which is: $\boldsymbol{\omega_L} = \gamma \mathbf{B}$.

It is convenient to define a rotating reference frame, in which this frame is rotating with an arbitrary angular frequency $\boldsymbol{\Omega}$ relative to the inertial frame (also called the laboratory frame). In this rotating reference frame, the equation of motion of the magnetic moment is [108, p. 12]:

$$\frac{\delta \boldsymbol{\mu}}{\delta t} = \boldsymbol{\mu} \times \gamma(\mathbf{B} + \boldsymbol{\Omega}/\gamma) \tag{8.3}$$

In which the symbol $\delta/\delta t$ represents the time derivative in the rotating reference frame. Note that now the magnetic field $\mathbf{B}$ is in terms of the rotating reference frame coordinates. This equation is similar to equation 8.2 by replacing the magnetic field with an effective magnetic field: $\mathbf{B_{eff}} = \mathbf{B} + \boldsymbol{\Omega}/\gamma$. Therefore the magnetic moment is precessing around the effective magnetic field $\mathbf{B_{eff}}$ in the rotating reference frame. This rotating reference frame description is convenient when time varying magnetic fields are used, since a varying magnetic field appears to be static when the reference frame rotates with the angular rotation of the varying magnetic field. From equation 8.3, we see that the magnetic moment is static in the rotating reference frame ($\frac{\delta \boldsymbol{\mu}}{\delta t} = 0$) when the direction and amplitude of the angular frequency matches to the Larmor frequency ($\boldsymbol{\Omega} = -\boldsymbol{\omega_L} = -\gamma \mathbf{B}$).

## 8.2 Time varying magnetic field

By applying a time varying magnetic field $\mathbf{B_1}(t)$, which can be achieved by sending radio frequent (RF) waves, one can influence the magnetic moment of spins. In the laboratory frame, the equation of motion of a magnetic moment will be:

$$\frac{d\boldsymbol{\mu}}{dt} = \boldsymbol{\mu} \times \gamma(\mathbf{B} + \mathbf{B_1}(t)) \tag{8.4}$$

In the rotating reference frame, the time dependence of the $\mathbf{B_1}$ field can be dropped when the varying magnetic field is rotating with $\boldsymbol{\Omega}$. To prevent $\mathbf{B}$ to get a time

dependence in terms of the new coordinates, $\mathbf{\Omega}$ needs to be parallel to $\mathbf{B}$. This means that $\mathbf{B_1}$ will be perpendicular to $\mathbf{B}$. Therefore in the rotating reference frame:

$$\frac{\delta \boldsymbol{\mu}}{\delta t} = \boldsymbol{\mu} \times \gamma(\mathbf{B} + \mathbf{\Omega}_{\parallel \mathbf{B}}/\gamma + \mathbf{B}_{\mathbf{1} \perp \mathbf{B}}) \tag{8.5}$$

Most of the processes in magnetic resonance are described in the rotating reference frame, rotating with the $\mathbf{B_1}$ field.

## 8.3 Sending an RF field

Suppose, a radio frequent field is sent in the x-direction (laboratory frame) and the external magnetic field is pointing along the z-direction. Then the magnetic field from this electromagnetic wave can have the following form: $\mathbf{B_x} = 2B_1 cos(\omega t)\hat{\mathbf{x}}$, which can be decomposed into a left rotating $\mathbf{B_L}$ and right rotating field $\mathbf{B_R}$:

$$\mathbf{B_x} = \mathbf{B_L} + \mathbf{B_R} \tag{8.6}$$

$$\begin{aligned} \mathbf{B_R} &= B_1(cos(\omega t)\hat{\mathbf{x}} + sin(\omega t)\hat{\mathbf{y}}) \\ \mathbf{B_L} &= B_1(cos(\omega t)\hat{\mathbf{x}} - sin(\omega t)\hat{\mathbf{y}}) \end{aligned} \tag{8.7}$$

Where $2B_1$ is the amplitude and $\omega$ is the angular frequency of the radio frequent field. From equation 8.7, we see that $\mathbf{B_L}$ interchanges with $\mathbf{B_R}$ by replacing $\omega$ by $-\omega$. Therefore, when $\mathbf{B_R}$ is at resonance, the influence of $\mathbf{B_L}$ is negligible and vice versa, since the difference in angular frequency is $2\omega$. By defining an angular frequency $\omega_z$ which can be positive or negative, the rotating magnetic field will be:

$$\mathbf{B_1} = B_1(cos(\omega_z t)\hat{\mathbf{x}} + sin(\omega_z t)\hat{\mathbf{y}}) \tag{8.8}$$

Therefore $\mathbf{B_1}$ will become $\mathbf{B_L}$ or $\mathbf{B_R}$, depending on $\omega_z$. Using equation 8.4 with ($B_0$ in $\hat{z}$) we have:

$$\frac{d\boldsymbol{\mu}}{dt} = \boldsymbol{\mu} \times \gamma(B_0\,\hat{\mathbf{z}} + B_1 cos(\omega_z t)\hat{\mathbf{x}} + B_1 sin(\omega_z t)\hat{\mathbf{y}}) \tag{8.9}$$

The time dependence of $\mathbf{B_1}$ can be dropped in the rotating reference frame, where the coordinate system rotates about the z-direction with angular frequency $\omega_z$. Using equation 8.5, the motion of the magnetic moment will be:

$$\frac{\delta \boldsymbol{\mu}}{\delta t} = \boldsymbol{\mu} \times \gamma((B_0 + \omega_z/\gamma)\hat{\mathbf{z}}' + B_1\hat{\mathbf{x}}') \tag{8.10}$$

Where $B_1$ is taken along the x-direction. By taking $\omega_z = -\omega$, we see that the resonance condition for equation 8.10 will be $\omega = \gamma B_0$ for positive $\gamma$. In this case the left rotating field component of the radio frequent field causes the resonance for positive $\gamma$. The motion of the magnetic moment in the rotating reference frame, rotating with $-\omega$, is therefore [108, p. 21]:

$$\frac{\delta \boldsymbol{\mu}}{\delta t} = \boldsymbol{\mu} \times \gamma \mathbf{B_{eff}} \tag{8.11}$$

$$= \boldsymbol{\mu} \times \gamma((B_0 - \omega/\gamma)\hat{\mathbf{z}}' + B_1\hat{\mathbf{x}}') \tag{8.12}$$

## 8.4 Common RF pulses

In the following part we will describe pulses that are used in NMR and MRI. Again, we assume that initially the magnetic moment $\mu$ is pointed along the external magnetic field $B_0\hat{\mathbf{z}}$ in the z-direction. In resonance ($\omega = \gamma B_0$), the magnetic moment is precessing around $B_1\hat{\mathbf{x}}'$ in the rotating reference frame. Therefore the z-component of the magnetic moment is oscillating between positive z and negative z, with a frequency $\omega_1 = \gamma B_1$, called the Rabi- or nutation frequency. In the laboratory frame, the tip of the vector of the magnetic moment describes a spherical spiral around the z-axis. When the magnetic field is off-resonance, we see that the effective field, around which the magnetic moment is precessing, receives a z-component. In this case, the magnetic moment cannot reach the full magnitude along $\hat{\mathbf{z}}$. It is important to note however that off-resonant excitation does excite the spins. As a rule of thumb, it helps to keep in mind that the width of a peak in an NMR spectrum has a width (at full width half maximum (FWHM)) that is at least as wide as twice the $B_1$ field, $\delta\omega_{FWHM} = 2\gamma B_1$.

Any rotation $\theta$, relative to the z-axis of the magnetic moment can be achieved by sending a resonance RF pulse with amplitude $B_1$ for a duration of $\tau = \theta/(\gamma B1)$. The magnetic moment will be rotated to the transverse plane when a so-called $\pi/2$-pulse or 90 degree pulse is applied. A 180 degree rotation of the magnetic moment is called the $\pi$-pulse or inversion pulse.

## 8.5 Adiabatic inversion

In conventional MRI and NMR, $\pi/2$-pulses and $\pi$-pulses are commonly used. However, for MRFM applications these pulses are less convenient for several reasons: First, due to the demand of low dissipation and high power RF sources, generally these sources do not generate a homogeneous $B_1$ field, which makes $\pi/2$ and $\pi$-pulses unsuitable because different positions in the sample require to have different pulse widths. The second argument will be made clear in the following: In MRFM, the signal to noise ratio increases if the spin has a force interaction with the cantilever (force sensor). This force interaction is achieved by driving the spins in resonance with the cantilever. If one tries to drive the cantilever with Rabi-oscillations (continuous $\pi$-pulses), the $B_1$ field should be homogeneous and the Rabi frequency should exactly match the cantilever frequency ($\omega_c$): $\gamma B_1 = \omega_c$.

When performing adiabatic pulses, on the other hand, the sweep time of the adiabatic pulses determines the time of inversion. Therefore, one can achieve exactly timed adiabatic inversions as long as the adiabatic condition is fulfilled: $\omega_c \ll \gamma B_1$, which will be described later. Finally, due to the inhomogeneous $B_0$-field, the resonance slice thickness is more easily controlled by performing adiabatic pulses.

In the following, an adiabatic pulse will be described, in the rotating reference frame.

The magnetic moment can be inverted when the frequency of the $B_1$ field is swept from far below resonance to far above resonance. For convenience, assume that initially the magnetic moment $\mu$ is pointed along the external magnetic field $B_0\hat{\mathbf{z}}$ in the z-direction and assume that $B_1 \ll B_0$. Note that the description below

is also valid for a magnetic moment which is initially in the opposite direction. A magnetic moment, which is parallel to the effective field, is called *spin locked*. Likewise a magnetic moment, antiparallel to the effective magnetic field, is called *spin anti-locked*. Starting with a frequency of the $B_1$ field below resonance, the direction of the effective magnetic field and therefore the direction of the magnetic moment will alter only slightly. Moreover, the z-component of the effective magnetic field is dominant off-resonance, (assuming that $B_1 \ll B_0$).

We see that the effective field $\mathbf{B_{eff}}$ rotates about the y-axis in the rotating reference plane as the frequency approaches resonance, see 8.12. Using equation 8.12, the magnitude of $\mathbf{B_{eff}}$ and the angle $\alpha$ between the z-axis and $\mathbf{B_{eff}}$ is:

$$B_{eff} = \sqrt{(B_0 - \omega(t)/\gamma)^2 + B_1(t)^2} \tag{8.13}$$

$$\alpha = \arctan\left(\frac{B_1(t)}{B_0 - \omega(t)/\gamma}\right) \tag{8.14}$$

We have kept the frequency $\omega$ and $B_1$ time-dependent, since adiabatic inversion described below requires a frequency and amplitude modulation. From these equations, we see that a sweep of the $B_0$ field can have the same effect as a frequency sweep of $\omega$. Therefore an adiabatic inversion can equally well be performed by both methods.

It is now convenient to introduce another reference frame, in which the z-axis follows $\mathbf{B_{eff}}$ in the rotating reference frame, also called the $B_eff$-frame, as in ref. [117]. Therefore we obtain a doubly rotating reference frame, which rotates with $\omega_a = \frac{d\alpha}{dt}$ about the $\hat{\mathbf{y}}'$-axis. Hence, the motion of the magnetic moment in this reference frame is:

$$\frac{\tilde{\delta}\boldsymbol{\mu}}{\tilde{\delta}t} = \boldsymbol{\mu} \times \gamma\left(B_{eff}\hat{\mathbf{z}}'' + (\omega_a/\gamma)\hat{\mathbf{y}}''\right) \tag{8.15}$$

In which the symbol $\tilde{\delta}/\tilde{\delta}t$ represents the time derivative in the doubly rotating reference frame. From this equation, it becomes clear that in the case of a fast inversion (a large $\omega_a$), the component in $\hat{\mathbf{y}''} = \hat{\mathbf{y}}'$-direction becomes significant. This means that, after an inversion pulse, the magnetic moment can have a component in the lateral direction, which therefore blurs the inversion. The magnetic moment only follows the effective magnetic field $\mathbf{B_{eff}}$, provided that:

$$\omega_a(t) \ll \gamma B_{eff} \ \forall t \tag{8.16}$$

Since $B_1 \ll B_0$, the minimal magntiude of the effective magnetic field is equal to $B_1$. Hence,

$$\omega_a(t) \ll \gamma B_1 \tag{8.17}$$

This is called the adiabatic condition. A full inversion can only be achieved if this adiabatic condition is fulfilled. In the previous description, we treated the spins as being isolated. However, the spins have interaction with their environment, i.e. spin-lattice interaction and spin-spin interaction. If the spin system applies to the Bloch equations [118], it is sufficient to add a condition in which the relaxation mechanisms due to the environmental interactions are negligible during the adiabatic inversion [18, p. 66] :

$$1/\omega_a(t) \ll T_1, T_2 \tag{8.18}$$

Combining this condition with the previous (Eq. 8.17) and since $T_2$ is usually much smaller than $T_1$ ($T_2 \ll T_1$):

$$\frac{1}{T_2} \ll \omega_a(t) \ll |\gamma B_1| \tag{8.19}$$

Since $T_2$ times can be very short, the necessary speed of the passage has caused the adiabatic inversion to be called 'adiabatic rapid passage' [18, p. 66]. However, for solids, this inequality is far too stringent with RF fields larger than the local field from neighboring spins. [18, p. 66] [119]. A hand-waving argument, according to Redfield et al. [119] is as follows: Suppose that the magnetization with magnitude ($M_1$) is initially in the direction of the RF field, then according to the Bloch equations, the magnetization will decay exponentially to zero in a time $T_2$. The work during this decay is equal to $M_1 B_1$. Since we assumed that $T_2 \ll T_1$, the energy (during $T_2$) can only come from the spin-spin energy. Therefore, for $B_{loc} \ll B_1$ and due to conservation of energy, the spin system is not able to acquire the entire energy ($M_1 B_1$) corresponding to the applied rotating field $B_1$, which means that the $T_2$ decay according to the Bloch equations is partially forbidden. As a result, the transverse decay for the component of the magnetization parallel to the $B_1$ field (say, x'-direction in the rotating frame) is rather in the order of the $T_1$ time [119] [18, p. 66 and p. 539-545]. Meanwhile, the transverse decay for the component of the magnetization perpendicular to the $B_1$ (y'-direction) still decays with the $T_2$ time according to the Bloch equations. Since the magnetization follows the effective field if the adiabatic condition is fulfilled, only a small contribution of the field is in the y-direction. For many experiments the following less stringent inequality can be applied [18, p. 66]:

$$\frac{1}{T_1} \ll \omega_a(t) \ll |\gamma B_1| > |\gamma B_{loc}| \simeq \frac{1}{T_2} \tag{8.20}$$

Where $B_{loc}$ is the local magnetic field experienced by neighboring spins.

Many pulse shapes are used with several different forms of $\omega(t)$ and $B_1(t)$ [18, 117, 120, 121]. Most of the pulses will also give a time dependence of $B_{eff}(t)$ and $\omega_a(t)$. However, we can try to find a time independent solution by requiring that $dB_{eff}/dt = 0$ and $\omega_a = d\alpha/dt$ is constant. The latter requirement ensures a constant angular velocity of the effective field vector. Then, using equations 8.13 and 8.14 and taking $\omega(t) = \gamma B_0 + \Delta\omega(t)$, we find the following differential equations:

$$0 = B_1(t)\dot{B}_1(t) - \frac{\Delta\omega(t)\Delta\dot{\omega}(t)}{\gamma^2} \tag{8.21}$$

$$\omega_a = \frac{\dot{B}_1(t)\Delta\omega(t)/\gamma + B_1(t)\Delta\dot{\omega}(t)/\gamma}{B_1(t)^2 + \Delta\omega(t)^2/\gamma^2} \tag{8.22}$$

We take the boundary condition such that the spin is aligned to the external magnetic field (in z-direction) at t=0. This yields at resonance $\Delta\omega(\frac{\pi/2}{\omega_a}) = 0$ and $B_1(\frac{\pi/2}{\omega_a}) = B_{1_0}$. By solving the differential equations with the latter boundary conditions, we obtain a full adiabatic inversion with the following time dependencies of the $B_1$ field

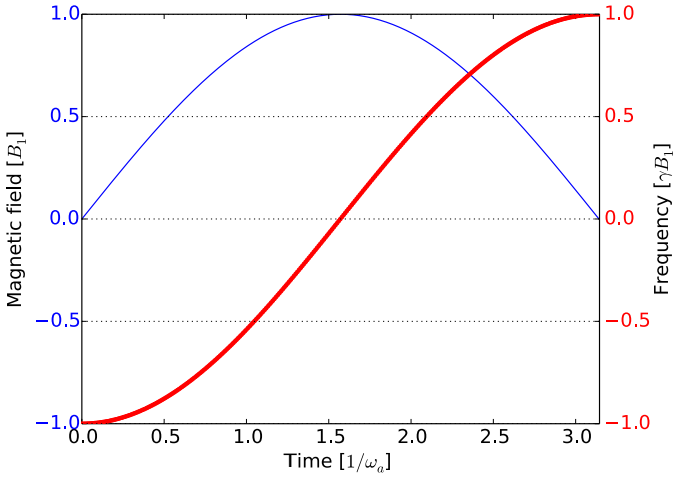


Figure 8.1: Adiabatic rapid passage in which the change in the magnitude of the effective field is zero and in which the tip of the effective field rotates with a constant angular velocity. The red curve corresponds with the frequency sweep of $\Delta\omega$ and the blue curve corresponds with the amplitude modulation of $B_1(t)$.

and angular frequency modulation ($\Delta\omega$):

$$B_1(t) = B_{1_0} \sin(\omega_a t) \quad 0 \leq t \leq \frac{\pi}{\omega_a} \tag{8.23}$$

$$\Delta\omega(t) = -\gamma B_{1_0} \cos(\omega_a t) \quad 0 \leq t \leq \frac{\pi}{\omega_a} \tag{8.24}$$

In figure 8.1, the adiabatic inversion pulse is shown. The same adiabatic inversion would have been obtained if we sweep the external magnetic field ($B_0^*(t)$) instead of $\Delta\omega(t)$, according to:

$$B_0^*(t) = B_0 + \Delta B_0 = B_0 + B_{1_0} \cos(\omega_a t) \quad 0 \leq t \leq \frac{\pi}{\omega_a} \tag{8.25}$$

Since $\omega_a$ is constant in these equations, the adiabatic condition without time dependence of $\omega_a$ applies for these pulse shapes (see Eq. 8.17).

Other pulse shapes are designed to be more independent of resonance offsets or they are designed to decrease the average or peak power of the RF-radiation. These so called offset independent adiabaticity (OIA) pulses are useful in NMR and MRI to obtain larger signals. In the case of MRFM, one would rather like to have small resonance slices, which omits the requirement of large offset independent pulses. However, it may still be of interest to control the resonance slice thickness with these pulses, to increase the signal to the desired level.In the following, we will evaluate a condition

for offset independent adiabaticity pulses [117]. If we apply the adiabatic condition (Eq. 8.16) with a resonance offset $\Omega$ incorporated, we obtain:

$$C(\Omega, t) = \frac{\gamma B_{eff}(t)}{\mathrm{d}\alpha(t)/\mathrm{d}t} \tag{8.26}$$

$$= \frac{\left((\Omega - \Delta\omega(t))^2 + \gamma^2 B_1^2(t)\right)}{\gamma \dot{B}_1(t)(\Omega - \Delta\omega(t)) + \gamma B_1(t)|\Delta\dot{\omega}(t)} \gg 1 \tag{8.27}$$

$$= \text{for } \ |\Omega| \leq \max(|\Delta\omega|) = A \tag{8.28}$$

Where A is the frequency sweep amplitude and C indicates how much the adiabatic condition is fulfilled. In order to obtain high independence of $\Omega$ in the bandwidth $A$, we can require that the condition must be equally satisfied for all $\Omega$. This means that C needs to be independent of $\Omega$, which is satisfied on resonance ($\Omega = \Delta\omega$) at time $t_\Omega$:

$$C(t_\Omega) = \frac{\gamma^2 B_1^2(t_\Omega)}{\Delta\dot{\omega}(t_\Omega)} \gg 1 \tag{8.29}$$

Therefore, we obtain an equation for which the condition satisfies equally well for all $|\Omega| \leq |A|$:

$$C(t_\Omega)\dot{\Delta\omega}(t_\Omega) = \gamma^2 B_1^2(t_\Omega) \tag{8.30}$$

Since at resonance, the effective field is only determined by $B_1$, which normally corresponds to the lowest effective field for $B_1 \ll B_0$, the adiabatic condition and Eq. 8.29 is most critical at $t_\Omega$. Therefore we can assume that usually Eq. 8.27 is satisfied for all $t$ within the pulse. The simplest RF pulse which satisfies Eq. 8.30 equally well for all $|\Omega| \leq A$, is a constant $B_1$ field and a linear frequency sweep. This pulse is often used in MRFM [2, 30, 122]. Therefore the condition in Eq. 8.29 is often shown as the adiabatic condition. Equation 8.30 assembles to Eq. 3.21 for a straight line frequency sweep: $\Delta\omega(t) = A\omega_a \frac{t}{2\pi} - \frac{1}{2}A$ and constant $B_1$, where $\omega_a = 2\pi/T_p$ with $T_p$ the pulse length.

From equations 8.23, 8.24 and 8.14, we see that the adiabatic rotation of the spin is only independent of the $B_1$ field if the rotation is 90 or 180 degrees. For in-plane rotations, such as performed in spin echo experiments, the end phase of an adiabatic in-plane inversion depends on the frequency and magnetic field. Since these are not constant during the pulse, the phases of the components of the magnetization will only slightly refocus after an in-plane rotation. This means that spin echo experiments yield poor results when performed by conventional adiabatic in-plane inversions. This effect can be impaired if a composite pulse like a $B_1$ insensitive rotation (BIR) pulse is used. This pulse will be described in the next section.

## 8.6 $T_2$ measurements with $B_1$ insensitive rotation (BIR)

In contrast to free induction decay as used in conventional nuclear magnetic resonance (NMR) and magnetic resonance imaging (MRI), in MRFM it is hard to measure the

spin-spin relaxation times ($T_2$ relaxation), since usually inhomogeneous $B_1$ fields are present. However, a lot of interesting information is buried in the $T_2$ relaxation times of materials.

In order to measure the $T_2$ relaxation times, one usually performs spin-echo experiments. The conventional way of performing spin-echo experiments is by applying a $\pi/2$ $\pi$ pulse (Hahn echo), in which the magnetization is transferred to the transverse plane where the dephasing occurs, whereupon the components of the magnetization can refocus after being inverted. This procedure only applies when the $B_1$ field is homogeneous over the sample, since otherwise the majority of spins would not make an exact $\pi/2$ or $\pi$ pulse. Moreover, in the case of spin-echo experiments for MRFM, the spins have to be transferred to the longitudinal direction after being dephased and refocused. As stated above, since usually in MRFM one has to deal with an inhomogeneous $B_1$-field, a spin echo has to be performed with an adiabatic pulse.

In the following, an adiabatic pulse sequence that is used in NMR and MRI will be described, which may be useful for future MRFM experiments in which spin-spin relaxation is relevant.

The pulse sequence and the schematic description of the pulse is shown in figure 8.2. First, the so called BIR-1 will be described, which is the more simple version of the later discussed BIR-4. Both pulses were introduced and described by Garwood et al. [123, 117] The basic idea is to perform an adiabatic pulse in which the dephasing and refocusing occurs due to a combination of a phase delay in the RF pulse and an inversion of the effective field. The phase delay determines the final rotation of the magnetization vector. The BIR-1 pulse consists of two segments and will be described in the rotating reference frame. Again, we assume that initially the magnetization vector is pointed in the z-direction, parallel to the external field.

The pulse starts with the effective field in the transverse plane in the x-direction (in resonance), whereupon the effective field is rotated to the z-axis by an adiabatic sweep. During this sweep the magnetic moment precesses perpendicularly around the effective field to the transverse plane. During this precession, dephasing occurs mainly due to inhomogeneities of the $B_1$- and $B_0$ field. After the end of this adiabatic pulse ($T_p/2$), the effective field is inverted by a sign change with magnitude $\Delta\omega$. At exactly the same moment ($T_p/2$) a phase shift of $\Delta\phi = \pi + \theta$ is introduced in which $\theta$ will be the final rotation of the magnetization. For a 90 degrees rotation, one therefore needs a 270 degrees phase shift of the RF pulse. During this event, the rotation direction of the precession changes (in the rotating reference frame), which means that the accumulated phase runs back and therefore refocuses the components of the magnetization. The phase shift causes the effective field to rotate to the -y-axis instead of the x-axis. Due to the symmetry of the pulse, which zeroes the accumulated phase when off-resonance effects are omitted, the magnetization vector ends on the transverse plane in the -x-direction.

In the case of a $B_0$ field inhomogeneity, yielding a resonance offset $\Omega$, the total accumulated phase may not be zero [117]:

$$\Psi_{tot} = \Psi_1 + \Psi_2 = -\int_0^{T_p/2} B_{eff}(t)\mathrm{dt} + \int_{T_p/2}^{T_p} B_{eff}(t)\mathrm{dt} \tag{8.31}$$

Where $B_{eff}$ is as Eq. 8.13, from which $\omega(t)$ is shown in figure 8.2. We can see from

the formulas and looking at figure 8.2, that the two integrals (corresponding to the two pulse segments) do not equal each other when a frequency offset is present. As an example, in the case of a positive resonance offset, the difference $\omega_0 - \omega(t)$ is smaller in the first integral than in the second.

This effect can be eliminated by the BIR-4 pulse as described below. Another effect, which cannot be compensated by the BIR-4 pulse but does not depend on the length of the pulse, is the fact that the initial effective magnetic field receives an angle, see Eq. 8.14. The BIR-4 pulse essentially consists of two concatenated BIR-1 pulses with four segments. In segment three, the pulse continues on BIR-1, in which the phase starts to increase (opposite to segment one). In between segment three and four, the effective field is inverted again, with an accompanied phase shift. In this way, the total phase is zero, since $-\Psi_1 = \Psi_3$ and $\Psi_2 = -\Psi_4$. With the BIR-4 pulse, two phase shifts have to be applied in accordance with:

$$\Delta\phi_1 = \pi + \theta/2 \tag{8.32}$$

$$\Delta\phi_2 = -\pi + \theta/2 \tag{8.33}$$

Where $\theta$ is the final rotation of the magnetization vector.
The effect of the spin-spin interaction becomes apparent when the short-lived interactions with other spins cause irreversible additional phases to the components of the magnetization. This eventually ends up in a dephased (smaller) magnetization vector. In a free induction decay experiment, this will be apparent after several spin-echo experiments with different delays between the $\pi/2$ and $\pi$ pulses.

In the case of a BIR-4 180 degree rotation, after dephasing and rotating the magnetization to the z-axis, a resultant smaller z component of the magnetization will be observed. Using different pulse lengths, in which the phase error increases with pulse length, a $T_2^*$ measurement may be performed. Another advantage of the BIR pulse is that any rotation of the magnetization can be performed adiabatically. Note that the $T_2$ relaxation time of the pulse may not be too short when the $B_1$ field is much smaller than the local field ($B_{loc}$), else all information may be lost already during one pulse, see Eq. 8.19 and Eq. 8.20.

## 8.7 Pulse sequences for MRFM: OSCAR and CERMIT

The pulse sequences that are described in this section are designed to invert spins in synchronization with the resonance frequency of the cantilever. In the following, the OScillation Cantilever-driven Adiabatic Reversals (OSCAR) and interrupted OSCAR (iOSCAR) will be described [124, 27]. When the cantilever is moving at its resonance frequency in the presence of a $B_1$-field, the dipolar field from the magnet sweeps its resulting resonance slice back and forth through the sample. This creates an oscillating $B_0$ field around the resonance slice. Looking at Eq. 8.13 and Eq. 8.14, the spins invert back and forth adiabatically. These inversions create a force which either repels or attracts the cantilever, depending on the relative position of the cantilever and the spins as well as on the orientation of the spins. The oscillating force changes

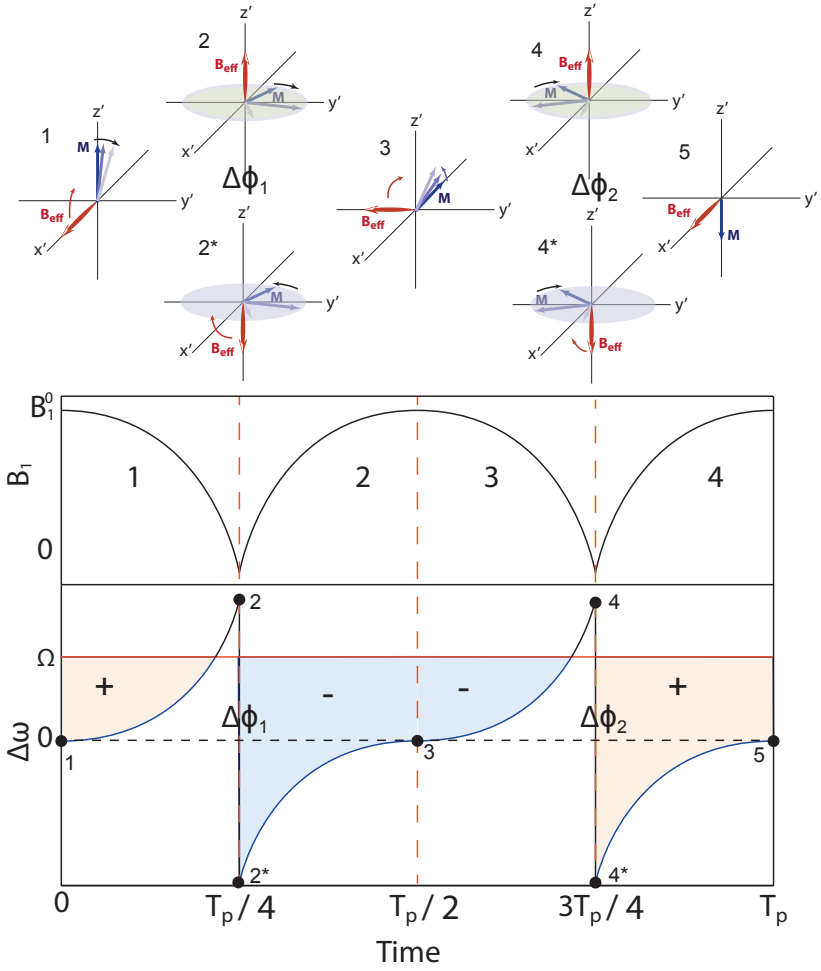


Figure 8.2: The pulse shape of a $B_1$ independent rotation in the case of a BIR-4 pulse. The simpler BIR-1 pulse, which does not compensate for resonance offsets $\Omega$, consists of just half the BIR-4 pulse with time $T_p/2$. The red dashed lines divide the pulse into 4 segments. On the upper side of the image, the accompanying representation of the pulse in the rotating frame is shown. In this representation, the evolution of the $B_{eff}$ field and the components of the magnetization (M) are shown for the events during the pulse, which are numbered from 1 to 5 and marked by black dots on the curve. Initially, the magnetization is supposed to be in the z'-direction (the accent marks the rotating frame representation). The effective field starts on resonance, and is chosen to be at the x' axis. The magnetization stays perpendicular to the effective field when the adiabatic condition is fulfilled. It rotates around the effective field with its corresponding frequency $\gamma B_{eff}$. Dephasing occurs mainly due to $B_1$ field inhomogeneity. The accumulated phase error refocuses again after the abrupt frequency step, in which the effective field changes sign. Due to an added phase shift of 270° between point 2 and 2*, the magnetization ends up in the transverse plane. The same procedure is repeated in segment 3 and 4 to undo the extra phase shift when a resonance offset $\Omega$ is present. The compensation of the accumulated phase error due to the offset can be seen by the filled areas, which are related to the accumulated phase error; segment 3 compensates segment 1 and segment 4 compensates segment 2 (at point 2 and 4, the phase accumulation is reversed).

the restoring force from the cantilever, shifting its effective spring constant [124]: $\Delta k = F_{spin}/\Delta z$.

In order to obtain a large and reproducible signal from the spins, the $B_1$ field is switched on at the maximum deflection of the cantilever. The frequency shift, which corresponds to the spring constant shift can be detected by a PLL-measurement or by frequency detection while self-oscillating the cantilever. The pulse is shown in figure 8.3a. As described in chapter 3 and chapter 6, surface noise, which is responsible for most of the 1/f noise at the eigenfrequency of the cantilever, is a major problem of this detection method. For this reason the iOSCAR protocol was introduced, in which the frequency shift is modulated. The protocol is shown in figure 8.3c. This protocol makes use of the fact that the shift of the spring constant changes sign, depending on the relative phase of the movement of the cantilever and the rotations of the spins.

In this protocol, the $B1$ field is switched off for half a cycle in every N cycles of the cantilever. During the off-cycle, the relative phase accumulates to a 180 degree phase shift, changing the sign of the frequency shift. The number of cycles (N) determines the frequency of the frequency shift changes: $f(\Delta f) = f_0/2N$. By the use of this protocol, the spin signal of a single electron was detected [27].

Another method, which is very similar to the OSCAR protocol, is the Cantilever Enabled Readout by Magnetization Inversion Transients (CERMIT) protocol [40], see figure 8.3b. In this protocol, the magnetization direction in the resonance slice determines the spring constant shift of the cantilever. Therefore this protocol is based on a different interaction than the OSCAR protocol. The advantage of this protocol is that instead of continuously driving the $B_1$ field, only one inversion is necessary to shift the resonance. This eventually lowers the power dissipation of the RF source, which will make it easier to reach lower temperatures.

Similar to the iOSCAR protocol, one can also modulate the frequency shift by cyclically inverting the spins, called cyclic CERMIT, see figure 8.3d. Practically, the pulse sequence is exactly the same as the iOSCAR protocol, but with the on and off state of the $B_1$ field interchanged. Both RF protocols are based on a response to a force gradient, changing the spring constant and therefore the frequency of the cantilever. However, the origin and amplitude of the force interaction are different.

## 8.8 Pulse sequences for MRFM: cyclic adiabatic driving

A force detection method is favorable, since it is more sensitive than frequency detection, as described in Chapter 3. This requires a method in which the cantilever is cyclically driven by the spins at the eigenfrequency of the cantilever, since static forces only shift the position of the cantilever. However, due to symmetry, when Boltzmann polarization is dominant, only a force from cyclic spin inversions is experienced by the cantilever when it is vibrating towards the surface (a cantilever with the long direction parallel to the surface). One of the first experiments with MRFM having this cantilever configuration was performed with cyclic saturation [125] and later on with cyclic adiabatic inversion [126]. This configuration is not favorable, since the cantilever may snap into contact with the surface, especially with the often used

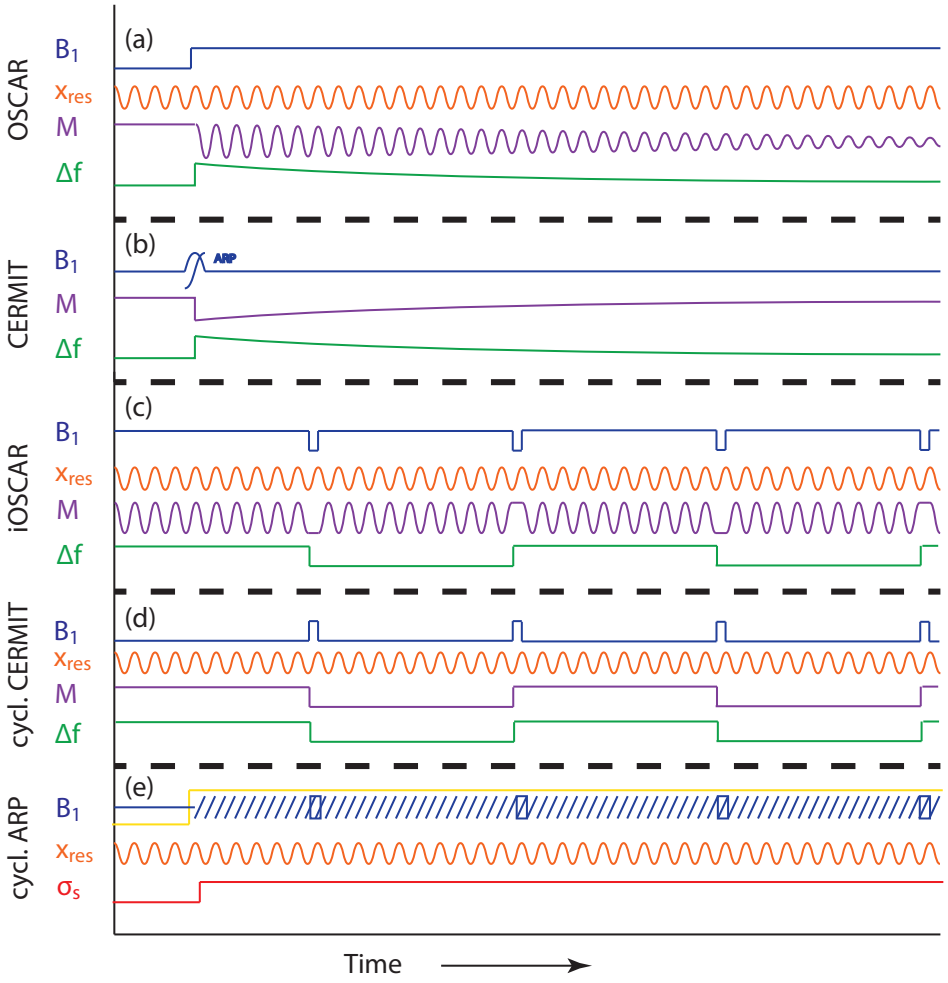


Figure 8.3: Radio frequency pulse sequences used in MRFM. (a) OScillation Cantilever-driven Adiabatic Reversals (OSCAR) pulse sequence. The motion of the magnetic particle on the cantilever ($x_{res}$) causes adiabatic inversions when the oscillating magnetic field ($B_1$) is switched on at a maximum of $x_{res}$. The oscillating magnetization $M$ causes a frequency shift $\Delta f$ on the frequency of the cantilever. (b) Cantilever Enabled Readout by Magnetization Inversion Transients (CERMIT). An adiabatic inversion causes a different spin configuration, changing the magnetization and the effective spring constant. (c) interrupted OSCAR (iOSCAR). By periodically switching off the $B_1$ field, a phase shift of $M$ corresponding to $x_{res}$ changes $\Delta f$ in synchrony. (d) cyclic CERMIT. By periodically applying adiabatic inversions, the frequency is shifted accordingly. (e) Cyclic adiabatic rapid passages. This pulse is applied for statistically polarized samples. By applying adiabatic inversions at twice the cantilever frequency, the spin inversions create a force on the cantilever depending on the configuration. The variance of these force interactions are translated into a variance $\sigma_s$ in the in phase component of the cantilever motion. To decrease measuring time, randomization pulses may be applied, which decrease the correlation of spin configurations (the squares in the $B_1$ field represent the randomization pulses).

floppy MRFM cantilever.

In the case of statistical polarization, a different cantilever orientation may still be used (perpendicular to the surface), since the force on the cantilever is dependent on the configuration of randomly oriented spins. The spin signal can be detected by using cyclic adiabatic pulses at twice the cantilever frequency while measuring the variance of the in-phase signal of the cantilever motion [2, 30, 122], see figure 8.3e. The doubling of the frequency of inversion pulses is required, because a full cycle of spins is obtained after two inversion cycles. This detection method was used for 3D imaging of virus particles with a resolution smaller than 10 nm [2].

A limiting factor, especially at low temperatures, is the required radio frequency current through the RF wire, due to the required fulfillment of the adiabatic condition in Eq. 8.17. The adiabatic condition in ref. [30] for fluorine with a gyromagnetic ratio of 40 MHz/T for a linear frequency sweep with a modulation amplitude of 1.4 MHz corresponding to Eq. 3.21 is equal to 1 if the $B_1$ field is 2 mT for a 6 kHz pulse frequency (2 times the cantilever frequency). Twice this $B_1$-field (4 mT) yields reasonable inversions [30]. Since only one of the rotating directions is in resonance (left rotating or right rotating, see section 8.3), the applied field has to be twice as large. This means that an oscillating magnetic field of 8 mT has to be sent (for a 4 mT $B_1$ field), which corresponds to an RF current of 20 mA for a sample at a distance of 500 nm from the RF wire such as in ref. [30].

In conclusion; although the force sensitivity increases signal-to-noise ratio, aspects such as cantilever orientation and RF current requirements limit the use of this method.

## 8.9 $T_1$ and $T_2$ measurements with a single adiabatic inversion

As described in the previous section and section 3.5, the necessary RF currents cause considerable heating, even when using a superconducting wire. In our current setup, the heating of the superconducting wire from the required current for cyclic adiabatic rapid passage is too much for measurements at millikelvin temperatures. However, we could perform a single and slower adiabatic passage to invert spins, such that the adiabatic condition 8.17 is satisfied more easily. On the other hand, when the $B_1$ field is lower than the local magnetic field ($B_{loc}$) we should take into account that the $T_2$ time should be large enough to fulfill the condition in Eq. 8.19. In the case of large RF fields, in the order of the local magnetic field or larger, the adiabatic rapid passage is limited by $T_1$, see Eq. 8.20 and section 8.5.

In the case of samples in which the spins carrying magnetic moments are close to each other (such as often the case in solids), the $T_2$ time may especially become short, since the $T_2$ time is approximately equal to the Larmor period from the local field of the neighboring spins [113, p. 14]. In the case of the copper sample, where the $T_2$ time is only 0.15 ms, a field larger than 500 $\mu T$ is enough to considerably increase the effective $T_2^*$ time. The required current at 1 $\mu m$ from the RF wire is therefore 5-10 mA. The length of the adiabatic pulse may then be much longer, i.e. a fraction of the $T_1$ time, being $T_1 = 1$ second to 20 seconds depending on the temperature ($T < 1$ K).

The use of slow adiabatic (rapid) passage on silicon is much more feasible, since the natural abundance of $^{29}$Si (having a magnetic moment) is only 4.6% [127], yielding a longer $T_2$ time through larger average neighbor distance. Moreover the $B_1$ field is easily larger than the local field. The $T_2$ time is measured to be 25 seconds for undoped natural silicon at room temperature [128, p. 427]. If this $T_2$ time is dominated by dipolar interactions, it is expected to have little change when going to lower temperatures. Since the $T_1$ time is very long especially at low temperatures, it may be interesting, for example to measure the $T_2$ time of $^{29}$Si by using the BIR-protocol (see section 8.6) [128, p. 427]. The $T_1$ time is more than 8 hours at low temperatures (10 K) [128, p. 427]. Any other diluted spin system may also be of interest for slow adiabatic passage.